

New physics effects on top quark spin correlation and polarization at the LHC: a comparative study in different models

Junjie Cao¹, Lei Wu² and Jin Min Yang²

¹ *Physics Department, Henan Normal University, Xinxiang 453007, China*

² *Key Laboratory of Frontiers in Theoretical Physics,
Institute of Theoretical Physics, Academia Sinica, Beijing 100190, China*

Abstract

Extensions of the Standard Model often predict new chiral interactions for top quark, which will contribute to top quark spin correlation and polarization in $t\bar{t}$ production at the LHC. In this work, under the constraints from the current Tevatron measurements, a comparative study of the spin correlation and polarization is performed in three new physics models: the minimal supersymmetric model without R-parity (RPV-MSSM), the third-generation enhanced left-right model and the axigluon model. We find that the polarization asymmetry may be enhanced to the accessible level in all these models while the correction to the spin correlation may be detectable in the axigluon model and the RPV-MSSM with λ'' couplings.

PACS numbers: 14.65.Ha, 14.80.Ly, 11.30.Hv

I. INTRODUCTION

Among the known elementary particles, top quark is distinguished for its excessively large mass and therefore often speculated to be sensitive to new physics. So far the Tevatron experiments have measured some of its properties such as the $t\bar{t}$ cross section $\sigma(t\bar{t})$ and the differential cross section in each bin of $t\bar{t}$ invariant mass $M_{t\bar{t}}$ [1]. While most of the measurements agree well with the Standard Model (SM) predictions, its forward-backward asymmetry shows moderate deviation [2] which may be a harbinger for new physics [3–7]. Although the Tevatron collider is still running to collect more data, the top quark measurement will be limited by its small statistics. The Large Hadron Collider (LHC), however, will copiously produce top quarks, which provides good opportunities to precisely measure top quark properties and also to probe new physics [8].

To explore new physics effects on top quark processes, the spin information of top quark may be utilized because top quark decays rapidly before forming any hadronic bound state and its spin information is thus preserved. Explicitly speaking, for the $t\bar{t}$ production at the LHC, top quark is not polarized at the leading order of the SM since the production proceeds mainly through the QCD interaction and the parity-violating electroweak contributions to the spin polarization is negligibly small [9]. But on the other side, some extensions of the SM may predict new parity-violating interactions of top quark which can enhance the polarization sizably [10, 11]. Therefore, the polarization asymmetry can serve as a sensitive probe to new physics. In association with the spin polarization, the spin correlation of t and \bar{t} in the $t\bar{t}$ production, which can be readily generated through the parity-conserving QCD interaction [12], may also be altered significantly by the new interactions and so can be used as an additional way to probe new physics [13].

In the popular minimal supersymmetric standard model (MSSM), the SUSY effect on top quark polarization in the $t\bar{t}$ production mainly arises from the radiative correction induced by the axial-vector couplings of gluinos and thus the effect is small [14]. In the general left-right models, since the predicted new neutral gauge bosons are usually at TeV scale and their mediated contributions to $t\bar{t}$ production do not interfere with corresponding QCD amplitudes [15], it is unlikely to induce sizable polarization effects on the $t\bar{t}$ production. In the extended color interaction models such as the topcolor model [16], the breaking of the new color gauge symmetry will give rise a massive octet coloron with strong coupling to top

quark. But due to its vector interaction nature with fermions, the coloron mainly affects the $t\bar{t}$ production rate instead of the polarization asymmetry [17]. Based on above observation, we investigate the top quark polarization asymmetry and the spin correlation between t and \bar{t} in the $t\bar{t}$ production at the LHC in another three models: the R-parity violating minimal supersymmetric standard model (RPV-MSSM), the third-generation enhanced left-right model (LR model) and the axigluon model. These models affect the $t\bar{t}$ production by exchanging at tree level the color-singlet sleptons (\tilde{l}_L^i) and/or the color-triplet squarks (\tilde{d}_R^k), the color-singlet vector boson Z' and the color-octet vector boson G' respectively. As shown below, although these effects on the $t\bar{t}$ production cross section may be quite small, they may be sizable in the top quark polarization and the spin correlation.

In our calculation, we take the SM parameters as [18]

$$m_t = 172.5 \text{ GeV}, m_Z = 91.19 \text{ GeV}, \sin^2 \theta_W = 0.2228, \alpha_s(m_t) = 0.1095, \alpha = 1/128, \quad (1)$$

and use the CTEQ6L1 [19] parton distribution function with the renormalization scale μ_R and the factorization scale μ_F set to be m_t . The following three quantities are considered:

- (i) The ratio P_t defined by [11]

$$P_t = \frac{(\sigma_{+-} + \sigma_{++}) - (\sigma_{--} + \sigma_{-+})}{\sigma_{+-} + \sigma_{++} + \sigma_{--} + \sigma_{-+}}, \quad (2)$$

where the polarization states for the \bar{t} quark (\pm denote the helicity) are summed over.

- (ii) The ratio A_{LR} defined by [11]

$$A_{LR} = \frac{\sigma_{+-} - \sigma_{-+}}{\sigma_{+-} + \sigma_{-+}}, \quad (3)$$

where the difference between helicity-unlike cross sections of $t\bar{t}$ pair is considered.

- (iii) The correction to the spin correlation of t and \bar{t} defined by [12]

$$\delta C = \frac{C_{tot} - C_{SM}}{C_{SM}} \quad (4)$$

where

$$C = \frac{(\sigma_{++} + \sigma_{--}) - (\sigma_{+-} + \sigma_{-+})}{\sigma_{++} + \sigma_{--} + \sigma_{+-} + \sigma_{-+}}. \quad (5)$$

In calculating these quantities, we have included the SM contribution. We require new physics predictions of $\sigma(t\bar{t})$ and $M_{t\bar{t}}$ at the Tevatron to coincide with their measured values at 2σ level [20, 21].

This paper is organized as follows. In Sec. II, III and IV we calculate the spin polarization and the spin correlation in the RPV-MSSM, the third-generation enhanced left-right model and the axigluon model respectively. We investigate the characteristics of the quantities in a comparative way. In Sec. V we discuss the observability of the quantities and then draw our conclusion.

II. SPIN POLARIZATION AND SPIN CORRELATION IN THE RPV-MSSM

The most general superpotential of the MSSM consistent with the SM gauge symmetry and supersymmetry contains R -violating interactions, which are given by [22]

$$\mathcal{W}_R = \frac{1}{2}\lambda_{ijk}L_iL_jE_k^c + \lambda'_{ijk}L_iQ_jD_k^c + \frac{1}{2}\lambda''_{ijk}\epsilon^{\alpha\beta\gamma}U_{i\alpha}^cD_{j\beta}^cD_{k\gamma}^c + \mu_iL_iH_2, \quad (6)$$

where i, j, k are generation indices, c denotes charge conjugation, α, β and γ are the color indices with $\epsilon^{\alpha\beta\gamma}$ being the total antisymmetric tensor, H_2 is the Higgs-doublet chiral superfield, and $L_i(Q_i)$ and $E_i(U_i, D_i)$ are the left-handed lepton (quark) doublet and right-handed lepton (quark) singlet chiral superfields respectively. The dimensionless coefficients λ_{ijk} (antisymmetric in i and j) and λ'_{ijk} in the superpotential are L -violating couplings, while λ''_{ijk} (antisymmetric in j and k) are B -violating couplings.

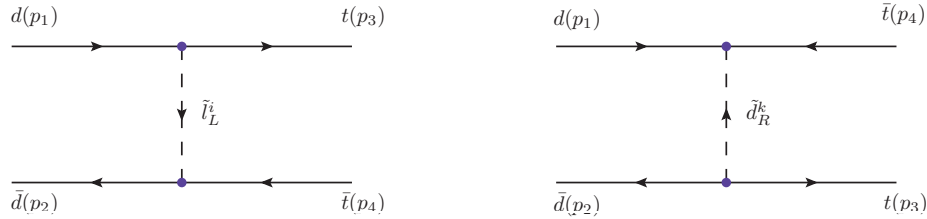


FIG. 1: Feynman diagrams contributing to $t\bar{t}$ production in the RPV-MSSM with \tilde{l}_L^i and \tilde{d}_R^k denoting i -th generation left-handed slepton and k -th generation right-handed squark respectively.

In Eq.(6) both λ' and λ'' terms can induce new chiral interactions of top quark, which, in terms of the four-component Dirac notation, are given by

$$\mathcal{L} = \lambda'_{ijk}\tilde{l}_L^i\overline{d}_R^k u_L^j - \frac{1}{2}\lambda''_{ijk}[\tilde{d}_R^{k*}\bar{u}_R^i d_L^{jc} + \tilde{d}_R^{j*}\bar{u}_R^i d_L^{kc}] + h.c. \quad (7)$$

TABLE I: The upper bounds on the couplings λ'_{i31} ($i = 1, 2, 3$) and λ''_{31k} ($k = 2, 3$) [24].

couplings	bounds	sources
λ'_{131}	$0.03 m_{\tilde{u}_L^i}/(100 \text{ GeV})$	$Q_W(Cs)$
λ'_{231}	$0.18 m_{\tilde{d}_L^k}/(100 \text{ GeV})$	$\nu_\mu q$
λ'_{331}	$0.26 m_{\tilde{d}_R^k}/(100 \text{ GeV})$	$K \rightarrow \pi \nu \bar{\nu}$
λ''_{31k}	$0.97 m_{\tilde{d}_R^k}/(100 \text{ GeV})$	R_l^Z
λ''_{31k}	1.25	perturbativity

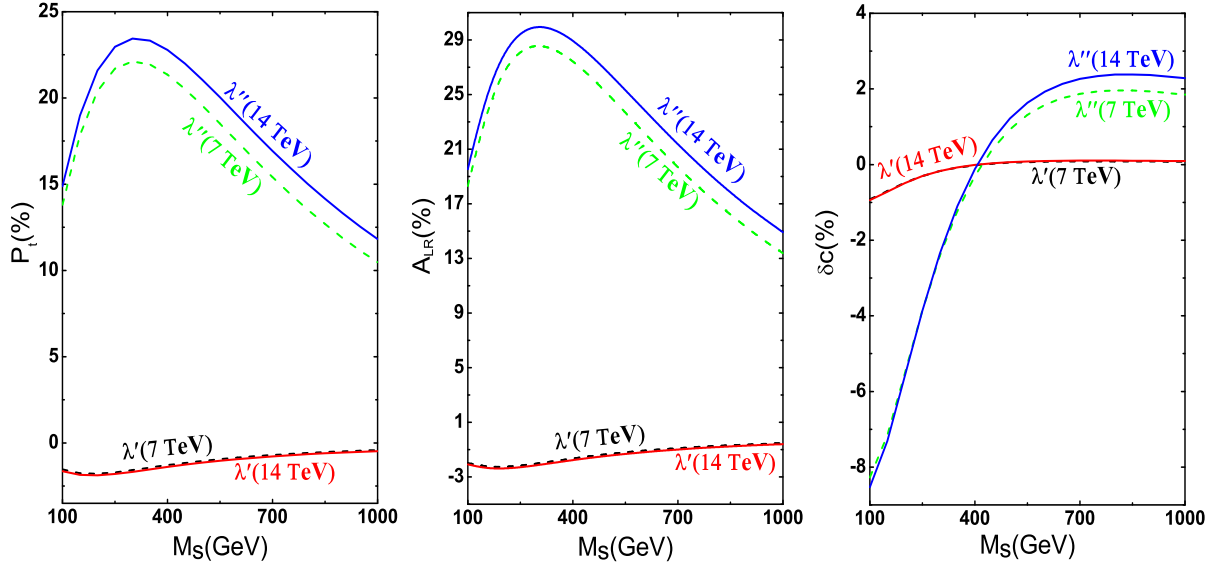


FIG. 2: The contributions of λ'_{i31} (lower curves) and λ''_{31k} (upper curves) to P_t , A_{LR} and δC at the LHC with $\sqrt{s}=7$ and 14 TeV, which are represented by the solid and dash lines.

These interactions contribute to the $t\bar{t}$ production by the diagrams shown in Fig.1 and their corresponding amplitudes are

$$M_{d\bar{d} \rightarrow t\bar{t}}^{RPV} |_{\lambda'} = -i\delta_{\alpha\rho}\delta_{\beta\sigma}|\lambda'_{i31}|^2 \frac{\bar{u}(t)P_R u(d)\bar{v}(d)P_L v(t)}{(p_1 - p_3)^2 - m_{\tilde{l}_{iL}}^2}, \quad (8)$$

$$M_{d\bar{d} \rightarrow t\bar{t}}^{RPV} |_{\lambda''} = -i\varepsilon_{\beta\rho\lambda}\varepsilon_{\sigma\alpha\lambda}|\lambda''_{31k}|^2 \frac{\bar{u}(t)\gamma_\mu P_R v(t)\bar{v}(d)\gamma^\mu P_R u(d)}{2[(p_1 - p_4)^2 - m_{\tilde{d}_{kR}}^2]}, \quad (9)$$

where $\alpha, \beta, \rho, \sigma$ and λ are color indices of the quarks and squarks and the sum over the generation indices i and k is assumed. Since the amplitudes depend on the coefficients λ'_{i31} and λ''_{31k} , to reasonably estimate the RPV-MSSM effect on the top pair production we consider their upper bounds from different measurements [23, 24], which are summarized in Table I. This table shows that the bounds are proportional to squark mass and for squark

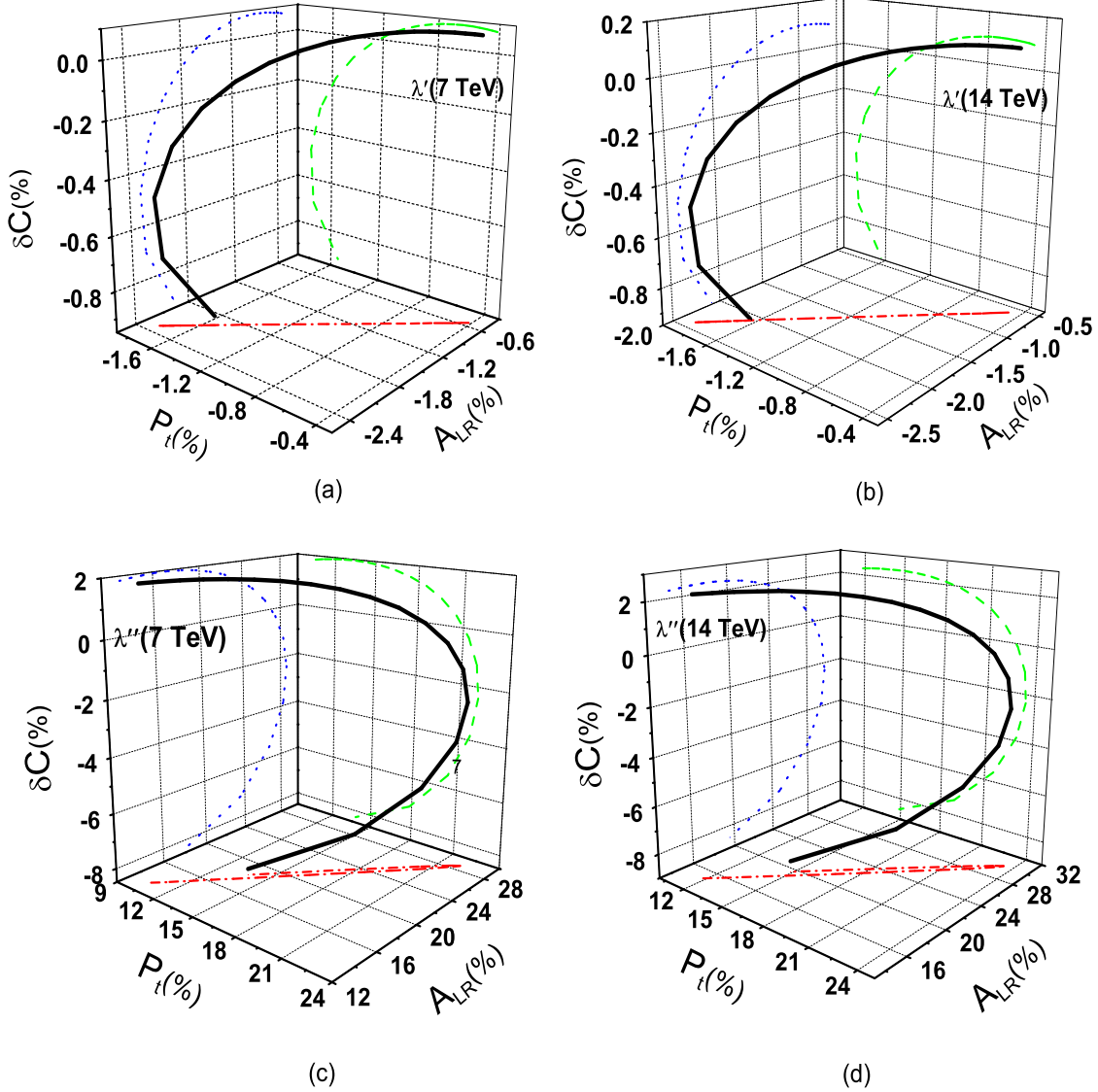


FIG. 3: The correlation among P_t , A_{LR} and δC for λ' and λ'' respectively at the LHC with $\sqrt{s}=7$ and 14 TeV. The projections(the blue, red and green lines) on different planes are also shown.

as heavy as 1 TeV, the coefficients may be of $\mathcal{O}(1)$. In our discussion, we assume all the squarks/sleptons degenerate in mass ($m_{\tilde{l}_L} = m_{\tilde{d}_R^k} = M_s$) and take the largest values of λ'_{i31} and λ''_{31k} for given M_s to maximize the RPV-MSSM effects. We require M_s larger than about 100 GeV, which corresponds to the mass bound from the LEP search for the sparticles [25].

Our results indicate that although the amplitudes interfere with the QCD amplitude $d\bar{d} \rightarrow g^* \rightarrow t\bar{t}$, their effects on the $t\bar{t}$ production cross section is only few percent [26] and thus unobservable at the LHC; but on the other hand, since the interactions violate parity, their effect on spin polarization may be sizable. The latter conclusion becomes obvious

from Fig.2 where we plot the three quantities P_t , A_{LR} , and δC versus M_s for the LHC with $\sqrt{s} = 7, 14$ TeV respectively. This figure shows that, due to the largeness of λ'' , the values of P_t , A_{LR} and δC can reach 23%, 30% and -8.5% respectively for $\sqrt{s} = 14$ TeV. In addition, we note that even if one further requires the RPV-MSSM to explain the top quark forward-backward asymmetry measured at the Tevatron at 2σ level, which favors the squark mass from 250 GeV to 400 GeV [5], the polarization asymmetry P_t and A_{LR} may still be tens percent and thus be observable at the LHC (see Table II in Sec. V).

Since in the RPV-MSSM, the three quantities depend on the same couplings, i.e. λ' or λ'' , their values should be correlated, which may be utilized to distinguish different models. In Fig.3 we show such correlation for λ' and λ'' , respectively. We see that the curves for λ' is very different from those for λ'' .

About the RPV-MSSM, two points should be noted. Although the coupling λ''_{31i} in the RPV model can be severely constrained by the $n - \bar{n}$ oscillation, the upper bound are dependent on the squark mass and other SUSY parameters, such as the chargino mass $m_{\tilde{w}}$ and the soft SUSY breaking parameters A_q . In the Ref.[3], they obtain the constraints for the scenario $m_{\tilde{q}} = m_{\tilde{w}} = A$, which is not relevant for our calculation. The other is we use the mass bounds of the sparticles from the LEP instead of from the Tevatron. The reason is we are considering R-parity violating case while the Tevatron results are valid only for the R-conserving case.

III. SPIN POLARIZATION AND SPIN CORRELATION IN THE LR MODEL

So far various left-right symmetric models have been proposed to understand the origin of parity violation and neutrino masses. These models generally predict new gauge bosons which contribute to $t\bar{t}$ production at tree level [15]. However, due to the heaviness of these bosons, they are hard to induce any significant effect on the $t\bar{t}$ production when the constraints from Tevatron are considered. Here we focus on a special left-right symmetric model called the third-generation enhanced left-right model, which still allows relatively light new gauge bosons and neutral flavor changing interaction at tree level [28]. This model is based on the gauge group $SU(3)_C \times SU(2)_L \times SU(2)_R \times U(1)_{B-L}$ with gauge couplings g_3 , g_L , g_R and g respectively, and the key feature of this model is the right-handed gauge bosons corresponding to $SU(2)_R$ group couple only to the third-generation fermions. After

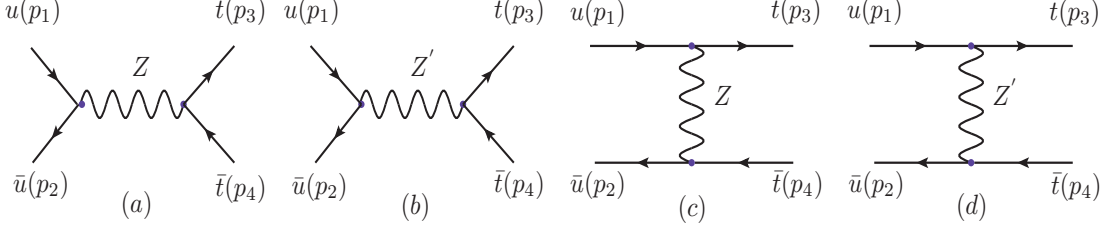


FIG. 4: Feynman diagrams contributing to $t\bar{t}$ production in the third-generation enhanced left-right model.

the mixings of the right handed bosons with the SM bosons and the light quarks in the SM with top quark, the $t\bar{t}$ production will be affected by the modified SM gauge interactions and also by additional contributions from new gauge bosons. In our analysis, we only consider the potentially large contribution from neutral gauge interactions, which are given by

$$\begin{aligned} \mathcal{L}_Z = & -\frac{g_L}{2\cos\theta_W}\bar{q}\gamma^\mu(g_V - g_A\gamma_5)q(\cos\xi_Z Z_\mu - \sin\xi_Z Z'_\mu) \\ & + \frac{g_Y}{2}\tan\theta_R(\frac{1}{3}\bar{q}_L\gamma^\mu q_L + \frac{4}{3}\bar{u}_{Ri}\gamma^\mu u_{Ri} - \frac{2}{3}\bar{d}_{Ri}\gamma^\mu d_{Ri})(\sin\xi_Z Z_\mu + \cos\xi_Z Z'_\mu) \\ & - \frac{g_Y}{2}(\tan\theta_R + \cot\theta_R)(\bar{u}_{Ri}\gamma^\mu V_{Rti}^{u*}V_{Rtj}^u u_{Rj} - \bar{d}_{Ri}\gamma^\mu V_{Rbi}^{d*}V_{Rbj}^d d_{Rj})(\sin\xi_Z Z_\mu + \cos\xi_Z Z'_\mu) \end{aligned} \quad (10)$$

where $\tan\theta_R = g/g_R$, $g_Y = g\cos\theta_R = g_R\sin\theta_R$, ξ_Z is the mixing angle between Z_R and Z_0 , q and q_L denote any quarks, $V_{Rij}^{u,d}$ are the unitary matrices which rotate the right-handed quarks u_{Ri} and d_{Ri} from interaction basis to mass eigenstates and the repeated generation indices i and j are summed.

Eq.(10) indicates that the $Z'\bar{u}_i u_j$ interaction is strong if $g_R \gg g_Y$ or equally $\cot\theta_R \gg 1$. In [28] nearly diagonal mixing matrices V_R^d and V_R^u were introduced to avoid large flavor-changing neutral currents. In practice, this requirement may be relaxed since sizable $u_R - t_R$ mixing with the other flavor mixings suppressed can still satisfy the constraints [4]. Here we emphasize that this pattern of flavor mixing does not necessarily mean the up-top element in up-type quark mass matrix M_u is much larger than other off-diagonal elements. For example, assuming $(V_R^u)_{ut} = 0.2$, $(V_R^u)_{ct} = 0$ and $(V_R^u)_{uc} = 0$, we numerically solve the equation $V_R^{u\dagger} M_u^\dagger M_u V_R^u = M_{diag}^2$ with $M_{diag}^2 = \text{diag}\{m_u^2, m_c^2, m_t^2\}$, and we find it possible that $(M_u)_{ct}$ is several times larger than $(M_u)_{ut}$. With the non-vanishing $u_R - t_R$ mixing, the top pair production may proceed by the t -channel diagrams shown in Fig.4 (c-d), and unlike the s -channel contribution in Fig.4 (a-b), this t -channel contribution will interfere with the QCD process $u\bar{u} \rightarrow g^* \rightarrow t\bar{t}$, so is more important than the s -channel contribution.

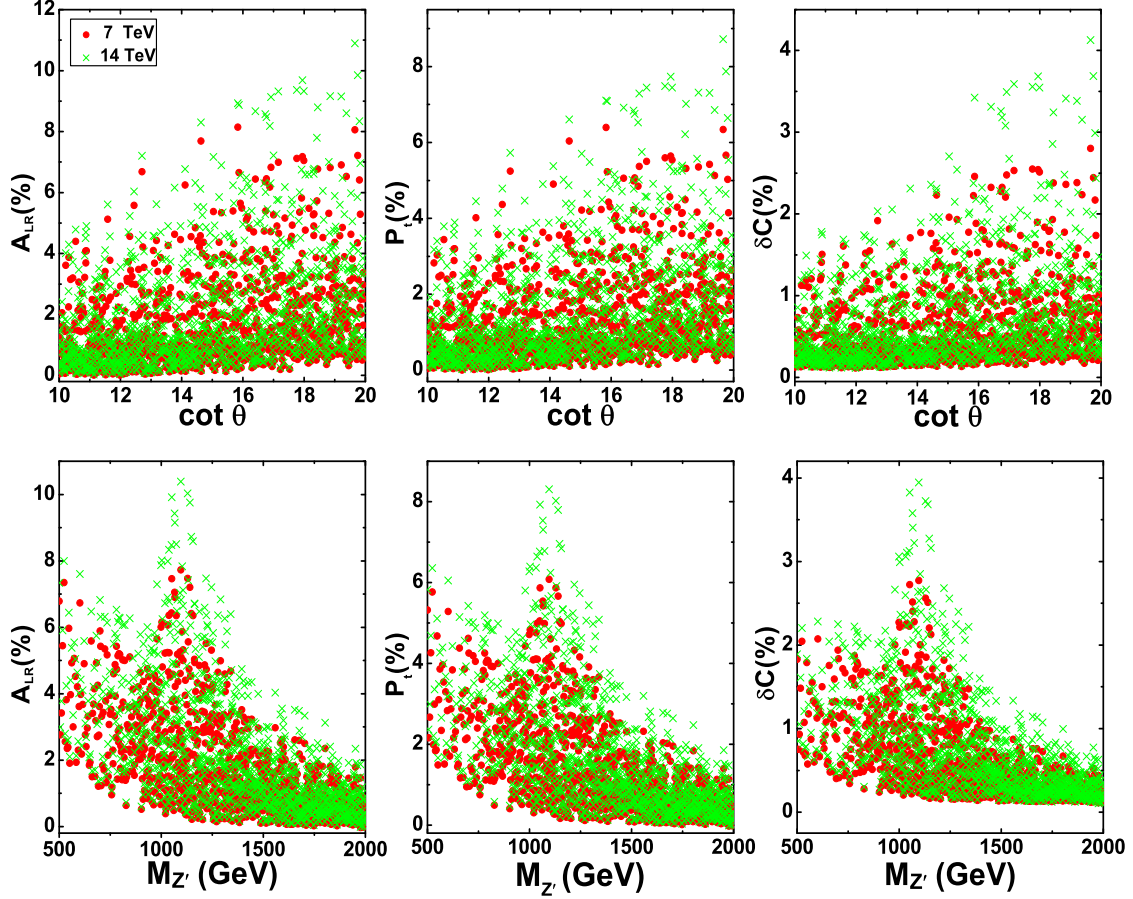


FIG. 5: Scatter plots of the quantities P_t , A_{LR} and δC as a function of $M_{Z'}$ or $\cot \theta_R$ in the LR model. Constraints from the Tevatron measurements on $\sigma(t\bar{t})$ and $M_{t\bar{t}}$ are imposed. The bullets (red) and crosses (green) denote respectively the center-of-mass energy $\sqrt{S} = 7$ TeV and 14 TeV at LHC.

The amplitudes corresponding to Fig.4 are given by

$$M_a = i\delta_{\alpha\beta}\delta_{\rho\sigma} \left(\frac{e}{2c_w s_w} \right)^2 \frac{\bar{u}(t)\gamma_\mu [g_{Z'L}^t P_L + g_{Z'R}^t P_R] v(t) \bar{v}(u)\gamma^\mu [g_{Z'L}^u P_L + g_{Z'R}^u P_R] u(u)}{(p_1 + p_2)^2 - m_Z^2}, \quad (11)$$

$$M_b = i\delta_{\alpha\beta}\delta_{\rho\sigma} \left(\frac{e}{2c_w s_w} \right)^2 \frac{\bar{u}(t)\gamma_\mu [g_{Z'L}^t P_L + g_{Z'R}^t P_R] v(t) \bar{v}(u)\gamma^\mu [g_{Z'L}^u P_L + g_{Z'R}^u P_R] u(u)}{(p_1 + p_2)^2 - m_{Z'}^2 - i\Gamma_{Z'} m_{Z'}}, \quad (12)$$

$$M_c = i\delta_{\alpha\rho}\delta_{\beta\sigma} \left(\frac{e}{2c_w s_w} \right)^2 [\xi_{Z s_w} (\cot \theta_R + \tan \theta_R)]^2 |V_{Rtu}^u V_{Rtt}^u|^2 \frac{\bar{u}(t)\gamma_\mu P_R u(u) \bar{v}(u)\gamma^\mu P_R v(t)}{(p_1 - p_3)^2 - m_Z^2}, \quad (13)$$

$$M_d = i\delta_{\alpha\rho}\delta_{\beta\sigma} \left(\frac{e}{2c_w s_w} \right)^2 [s_w (\cot \theta_R + \tan \theta_R)]^2 |V_{Rtu}^u V_{Rtt}^u|^2 \frac{\bar{u}(t)\gamma_\mu P_R u(u) \bar{v}(u)\gamma^\mu P_R v(t)}{(p_1 - p_3)^2 - m_{Z'}^2}, \quad (14)$$

where $\Gamma_{Z'}$ is the Z' width obtained by considering all decay channels of Z' , $s_w = \sin \theta_w$,

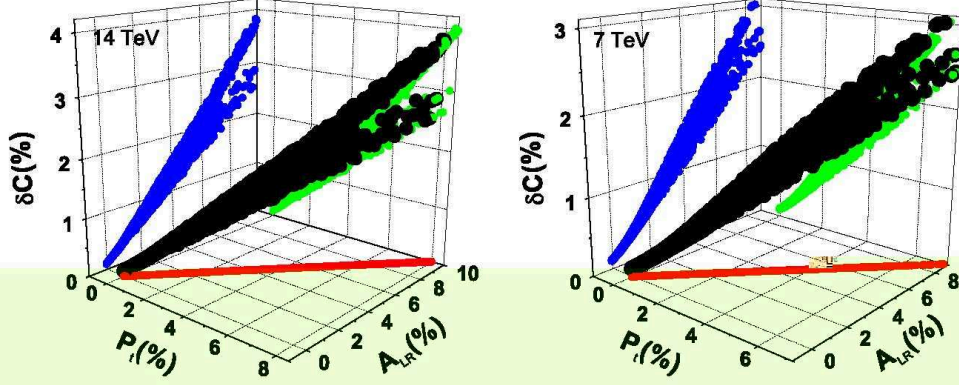


FIG. 6: Same as Fig.5, but showing the correlation of different polarization observables at the LHC with $\sqrt{s}=7$ and 14 TeV. The projections (the blue, red and green dots) on different planes are also shown.

$c_w = \cos \theta_w$, and the coupling coefficients $g_{ZL}^{t,u}$, $g_{ZR}^{t,u}$, $g_{Z'L}^{t,u}$ and $g_{Z'R}^{t,u}$ are defined as

$$g_{ZL}^{t,u} = 1 - \frac{4}{3}s_w^2 - \frac{1}{3}s_w \tan \theta_R \xi_Z, \quad (15)$$

$$g_{ZR}^u = -\frac{4}{3}s_w^2 - \frac{4}{3}s_w \tan \theta_R \xi_Z, \quad (16)$$

$$g_{ZR}^t = -\frac{4}{3}s_w^2 - \frac{1}{3}s_w \tan \theta_R \xi_Z + s_w \cot \theta_R \xi_Z, \quad (17)$$

$$g_{Z'L}^{t,u} = (1 - \frac{4}{3}s_w^2)\xi_Z + \frac{1}{3}s_w \tan \theta_R, \quad (18)$$

$$g_{Z'R}^u = -\frac{4}{3}s_w^2 \xi_Z + \frac{4}{3}s_w \tan \theta_R, \quad (19)$$

$$g_{Z'R}^t = -\frac{4}{3}s_w^2 \xi_Z + \frac{1}{3}s_w \tan \theta_R \xi_Z - s_w \cot \theta_R. \quad (20)$$

The amplitudes in Eq.(11-14) involve the parameters ξ_z , $\cot \theta_R$, $M_{Z'}$ and $(V_R^u)_{ut}$. About the parameters ξ_Z and $m_{Z'}$, the oblique T parameter and perturbative requirement will give constraints on ξ_Z (versus $m_{Z'}$) [28]. However, such constraints are obtained under the requirement to explain the b -quark forward-backward asymmetry A_{FB}^b , which, of course, can be relaxed if we give up the explanation of A_{FB}^b . Furthermore, for the $t\bar{t}$ productions, the main contributions are independent of the parameter ξ_Z [6]. Therefore, the constraints from the T parameter are almost irrelevant to our numerical study. We note that the constraints from CDF search for Z' [29] and from the global fitting of the electroweak precision data [30] are invalid here since these constraints arise mostly from the processes involving the fermions of the first two generations. So far the most pertinent bound comes from $e^+e^- \rightarrow b\bar{b}$ at LEP-II, which requires $M_{Z'} \gtrsim 460$ GeV for $\cot \theta_R \geq 10$ [28]. In our numerical calculation, we

scan over following parameter regions:

$$500 \text{ GeV} \leq M_{Z'} \leq 2000 \text{ GeV}, \quad 0 \leq \xi_Z \leq 0.02, \quad 10 \leq \cot \theta_R \leq 20, \quad 0.1 \leq (V_R^u)_{ut} \leq 0.2$$

Requiring the LR predictions for $\sigma(t\bar{t})$ and $M_{t\bar{t}}$ at Tevatron to coincide with their measured values at 2σ level, we display in Fig.5 the surviving samples on the planes of the polarization asymmetries versus $\cot \theta_R$ or $M_{Z'}$ respectively. This figure shows that large P_t , A_{LR} and δC come from the region where $\cot \theta_R$ is large. This can be understood by that in the LR model, the dominant contribution comes from the diagram (d) of Fig.4, which is proportional to $(\cot \theta_R + \tan \theta_R)^2$. This figure also shows that the samples with $500 < M_{Z'} < 900$ GeV affect little on the quantities. We checked that these samples are strongly constrained by the Tevatron measurements of $\sigma(t\bar{t})$ and $M_{t\bar{t}}$.

In Fig.6 we display the correlation of P_t , A_{LR} and δC for the surviving samples. We see that these three quantities are proportional to each other, which is quite different from the RPV-MSSM case.

Finally, we note that for most of the surviving samples, the top quark forward-backward asymmetry A_{FB} measured at the Tevatron lies within 2σ region around its experimental central value [5]. So even if we take the asymmetry as a constraint, our results for the spin polarization asymmetry still hold.

IV. SPIN POLARIZATION AND SPIN CORRELATION IN THE AXIGLUON MODEL

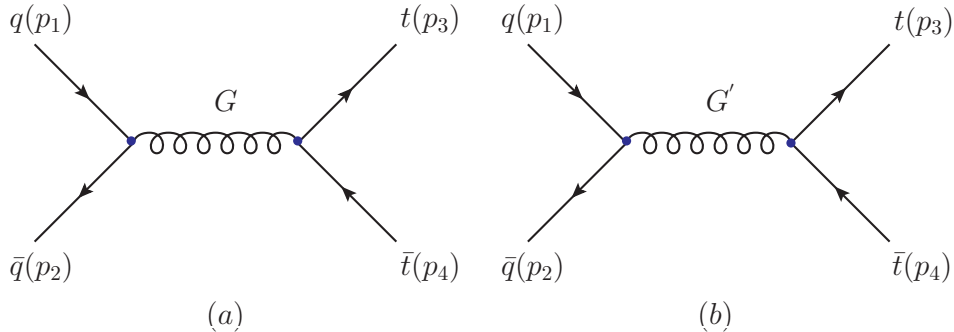


FIG. 7: Feynman diagrams contributing to $t\bar{t}$ production in the axigluon model with G and G' denoting gluon and axigluon respectively.

The third model we are considering is the chiral color model [31] which enlarges the

color group $SU(3)_C$ to $SU(3)_L \otimes SU(3)_R$ with gauge couplings g_L and g_R respectively. The spontaneous breaking of this enlarged symmetry to $SU(3)_C$ will produce massive color octet called axigluon. Depending on charge assignments of quarks under the $SU(3)_L \otimes SU(3)_R$ group, there are many variants of the chiral color models. In this paper, we focus on a special one which was utilized to explain the 2σ deviation of the top quark forward-backward asymmetry [6, 7]. The key feature of this model is the quarks in the third and the first two generations are assigned with different chirality in the $SU(3)_L \otimes SU(3)_R$ group, and consequently, the couplings of the axigluon with quarks are given by

$$g_V^q = g_V^t = -g_s \cot 2\theta, \quad g_A^q = -g_A^t = -g_s \csc 2\theta, \quad (21)$$

where θ is the rotation angle relating gluon G and axigluon G' to the interaction eigenstates G_1 and G_2 by

$$G = \cos \theta G_1 + \sin \theta G_2, \quad G' = \sin \theta G_1 - \cos \theta G_2. \quad (22)$$

The value of θ is determined by the gauge couplings, $\cot \theta = \tan^{-1}(g_L/g_R)$, and the perturbativity and the condition for fermion condensation require it vary from 14° to 45° .

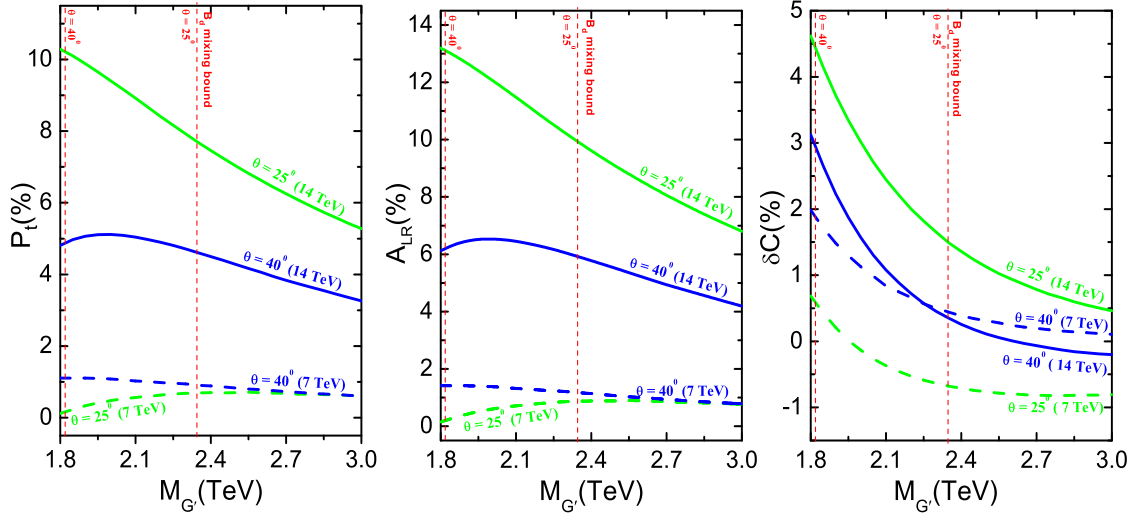


FIG. 8: The contribution of axigluon to top spin polarization and correlation at the LHC with $\sqrt{s}=7, 14$ TeV. The vertical dashed lines indicate the lower bounds on axigluon mass from $B_d - \bar{B}_d$ mixing [7].

In the axigluon model, the Feynman diagrams contributing to $t\bar{t}$ production are displayed

in Fig.7 and the corresponding amplitudes are

$$M_a = iT_{\beta\alpha}^a T_{\rho\sigma}^a g_s^2 \frac{\bar{u}(t)\gamma_\mu v(t)\bar{v}(q)\gamma^\mu u(q)}{(p_1 + p_2)^2}, \quad (23)$$

$$M_b = iT_{\beta\alpha}^a T_{\rho\sigma}^a \frac{\bar{u}(t)\gamma_\mu [g_V^t + g_A^t \gamma_5] v(t)\bar{v}(q)\gamma^\mu [g_V^q + g_A^q \gamma_5] u(q)}{(p_1 + p_2)^2 - m_{G'}^2 - i\Gamma_{G'} m_{G'}} \quad (24)$$

where g_s is the usual $SU(3)_C$ strong coupling, and $\Gamma_{G'}$ is the G' width obtained by assuming the axigluon decays only to the SM quarks [4, 6]. With the Tevatron constraints $\sigma(t\bar{t})$ and $M_{t\bar{t}}$, we show the dependence of P_t , A_{LR} and δC on $M_{G'}$ in Fig.8. This figure indicates that large predictions of these quantities come from the case of light G' and small θ , and for $\theta = 25^\circ$, $m_{G'} = 1.8\text{TeV}$ and $\sqrt{s} = 14\text{ TeV}$, P_t , A_{LR} and δC can reach 10.3%, 13.2% and 4.6% respectively.

Fig.8 shows that the magnitude of the effects is quite sensitive to the axigluon mass. About the axigluon mass, recently the direct search at the LHC gave a lower bound $m_{G'} > 1.52\text{TeV}$ [32], which, however, is for the flavor universal case and not applicable to our flavor non universal model. In Fig.8 we display an indirect bound $m_{G'} \sin(2\theta) > 1.8\text{ TeV}$ from the $B_d - \bar{B}_d$ mixing [7]. However, such a bound was derived under an assumption that the flavor mixing between the left-handed down-type quarks is approximated as the SM CKM matrix [33]. We see from Fig.8 that if we adopt such an assumption to impose this bound, then the axigluon effects will be rather limited.

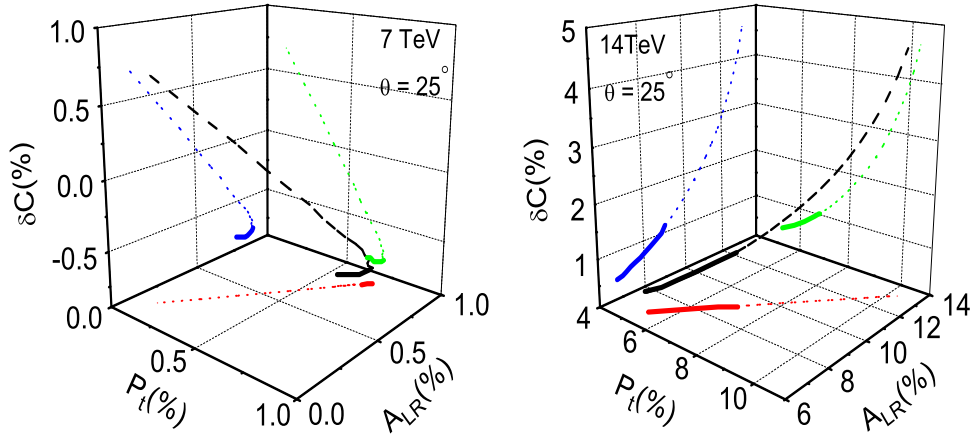


FIG. 9: The correlation among P_t , A_{LR} and δC in the axigluon model for the LHC with $\sqrt{s}=7,14$ TeV. Projections on different planes are also shown. For each curve, the solid part satisfies the lower bound on the axigluon mass from $B_d - \bar{B}_d$ mixing [7].

In Fig.9 we fix $\theta = 25^\circ$ and display the correlation of P_t , A_{LR} and δC at the LHC with

$\sqrt{s} = 7, 14$ TeV respectively. Comparing with the results in the RPV-MSSM with λ'' , we see that the three quantities have different correlation behavior.

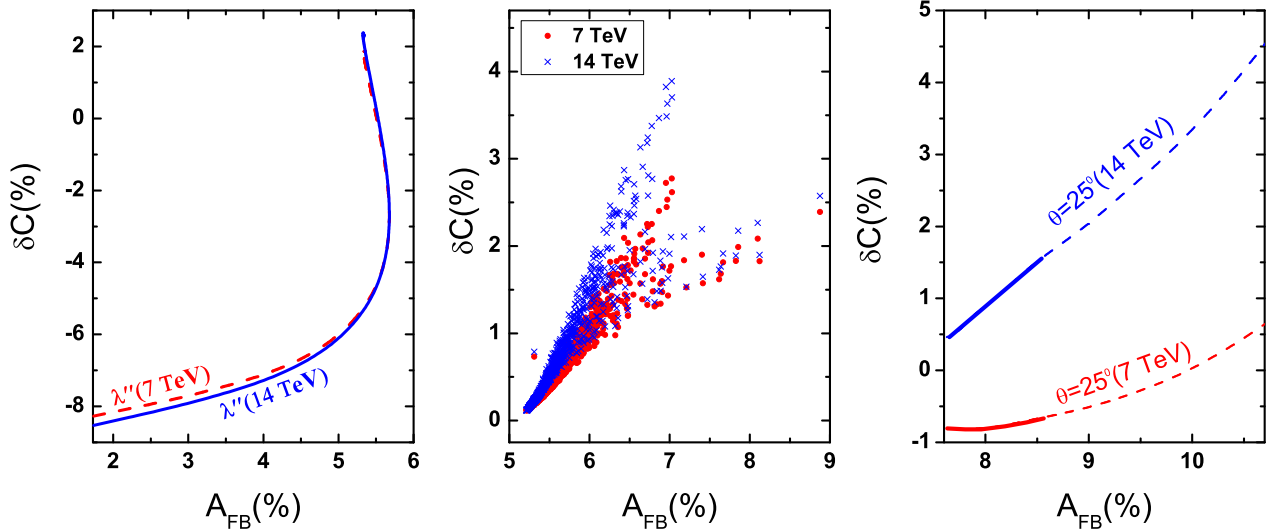


FIG. 10: The correlation between A_{LR} and δC in the λ'' , LR and axigluon models for the LHC with $\sqrt{s}=7, 14$ TeV. For the axigluon results displayed in the right frame, the solid part of each curve satisfies the lower bound on the axigluon mass from $B_d - \bar{B}_d$ mixing [7].

Finally, in Fig.10 we display the correlation between the spin correlation and the top quark forward-backward asymmetry in the λ'' RPV-MSSM, the LR and axigluon models, which can alleviate the A_{FB}^t deviation. It can be seen that the correlation behaviors are quite different for different models.

V. DISCUSSION AND CONCLUSION

In order to discuss the observability of the asymmetries P_t and A_{LR} , we calculate the statistical significance N_S defined in [11] and list their values in Table II for the optimum case of P_t and A_{LR} in the three models with an integrated luminosity $\mathcal{L} = 1 \text{ fb}^{-1}$. From the results of Fig.2,5,8 and Table II, we have following observations:

- (1) The LHC with $\sqrt{s} = 14 \text{ TeV}$ usually predicts larger N_S than that with $\sqrt{s} = 7 \text{ TeV}$. For the RPV-MSSM, the λ' -induced asymmetries are obviously unobservable at the LHC, while the λ'' -induced asymmetries may be detectable. For the specific left-right model and the axigluon model, P_t and A_{LR} may also be large enough to be detected at

TABLE II: The maximal statistical significance N_S (defined in [11]) for P_t and A_{LR} at the LHC with an integrated luminosity of 1 fb^{-1} .

	RPV-MSSM (λ')		RPV-MSSM (λ'')		LR Model (Z')		Axigluon Model (g')	
	P_t	A_{LR}	P_t	A_{LR}	P_t	A_{LR}	P_t	A_{LR}
7 TeV	1.7σ	1.9σ	29.1σ	36.5σ	8.8σ	9.9σ	1.71σ	1.95σ
14 TeV	3.1σ	3.5σ	59.2σ	68.3σ	18.4σ	20.6σ	26.5σ	32.8σ

the LHC. On the other hand, if the effects are not observed in the future, the stronger bounds can be imposed on the models.

- (2) Among the three models, the RPV MSSM and the axigluon model can allow for δC larger than 4% in magnitude, which may be observable at the LHC [34].

In summary, in this work we considered new physics effects on the top quark spin polarization and correlation at the LHC in three models: the RPV-MSSM, the specific left-right model and the axigluon model. We find that, due to the introduction of new parity-violating interactions of top quark, the polarization asymmetries P_t and A_{LR} can reach the observable level in all these models, while for the spin correlation the RPV MSSM and the axigluon model can cause observable effects at the LHC.

Acknowledgement

We thank Tao Han for discussions. This work was supported in part by HASTIT under grant No. 2009HASTIT004, by the National Natural Science Foundation of China (NNSFC) under grant Nos. 10821504, 10725526, 10635030, 10775039, 11075045 and by the Project of Knowledge Innovation Program (PKIP) of Chinese Academy of Sciences under grant No. KJCX2.YW.W10.

-
- [1] F. Deliot and D. Glenzinski, arXiv:1010.1202 [hep-ex]; M. A. Pleier, Int. J. Mod. Phys. A **24**, 2899 (2009); B. Stelzer, arXiv:1004.5368 [hep-ex]; A. Quadt, Eur. Phys. J. C **48**, 835 (2006).

- [2] G. Stricker *et al.*, CDF note 9724 (2009); T. Aaltonen *et al.* [CDF Collaboration], Phys. Rev. Lett. **101**, 202001 (2008); V. M. Abazov *et al.* [D0 Collaboration], Phys. Rev. Lett. **100**, 142002 (2008).
- [3] See, e.g., A. Djouadi, *et al.*, arXiv:0906.0604 [hep-ph]; O. Antunano, J. H. Kuhn and G. Rodrigo, Phys. Rev. D **77**, 014003 (2008); P. Ferrario and G. Rodrigo, Phys. Rev. D **78**, 094018 (2008); K. Cheung, W. Y. Keung and T. C. Yuan, arXiv:0908.2589 [hep-ph]; S. Jung, *et al.*, arXiv:0907.4112 [hep-ph]; J. Shu, T. Tait and K. Wang, arXiv:0911.3237 [hep-ph]; A. Arhrib, R. Benbrik and C. H. Chen, arXiv:0911.4875 [hep-ph]; D. W. Jung, P. Ko, J. S. Lee and S. h. Nam, Phys. Lett. B **691**, 238 (2010) I. Dorsner, *et al.*, arXiv:0912.0972 [hep-ph]; V. Barger, W.-Y. Keung, C.-T. Yu, Phys. Rev. D **81**, 113009 (2010); C. H. Chen, G. Cvetcic and C. S. Kim, arXiv:1009.4165 [hep-ph]; M. V. Martynov and A. D. Smirnov, Mod. Phys. Lett. A **25**, 2637 (2010); J. A. Aguilar-Saavedra, Nucl. Phys. B **843**, 638 (2011); C. Degrande, *et al.*, arXiv:1010.6304 [hep-ph]; B. Xiao, Y. k. Wang and S. h. Zhu, arXiv:1011.0152 [hep-ph]; arXiv:1006.2510 [hep-ph].
- [4] S. Jung, H. Murayama, A. Pierce and J. D. Wells, Phys. Rev. D **81**, 015004 (2010).
- [5] J. Cao, *et al.*, Phys. Rev. D **81**, 014016 (2010);
- [6] P. H. Frampton, J. Shu and K. Wang, arXiv:0911.2955 [hep-ph];
- [7] R. S. Chivukula, E. H. Simmons, C.-P. Yuan, arXiv:1007.0260 [hep-ph].
- [8] For top quark reviews, see, e.g., W. Bernreuther, J. Phys. G **35**, 083001, (2008) D. Chakraborty, J. Konigsberg, D. Rainwater, *Ann. Rev. Nucl. Part. Sci.* **53**, 301 (2003); E. H. Simmons, hep-ph/0211335; C.-P. Yuan, hep-ph/0203088; S. Willenbrock, hep-ph/0211067; M. Beneke, *et al.*, hep-ph/0003033; T. Han, arXiv:0804.3178; For model-independent new physics study, see, e.g., C. T. Hill and S. J. Parke, Phys. Rev. D **49**, 4454 (1994); K. Whisnant, *et al.*, Phys. Rev. D **56**, 467 (1997); J. M. Yang, B.-L. Young, Phys. Rev. D **56**, 5907 (1997); K. Hikasa, *et al.*, Phys. Rev. D **58**, 114003 (1998); J. A. Aguilar-Saavedra, arXiv:0811.3842; R.A. Coimbra, *et al.*, arXiv:0811.1743.
- [9] W. Beenakker, *et al.*, Nucl. Phys. B **411**, 343 (1994); C. Kao, G. A. Ladinsky and C. P. Yuan, Int. J. Mod. Phys. A **12**, 1341 (1997).
- [10] C. Kao, Phys. Lett. B **348**, 155 (1995); C. S. Li, R. J. Oakes, J. M. Yang and C. P. Yuan, Phys. Lett. B **398**, 298 (1997); S. Gopalakrishna, *et al.*, arXiv:1008.3508 [hep-ph]. R. M. Godbole, *et al.*, arXiv:1010.1458 [hep-ph].

- [11] C. Kao and D. Wackerroth, Phys. Rev. D **61**, 055009 (2000); K. Hikasa, J. M. Yang and B. L. Young, Phys. Rev. D **60**, 114041 (1999); P. Y. Li, *et al.*, Eur. Phys. J. C **51**, 163 (2007).
- [12] For top spin correlation in the SM, see, e.g., J. H. Kuhn, Nucl. Phys. B **237**, 77 (1984); V. D. Barger, J. Ohnemus and R. J. N. Phillips, Int. J. Mod. Phys. A **4**, 617 (1989); G. Mahlon and S. J. Parke, Phys. Lett. B **411**, 173 (1997); Phys. Rev. D **53**, 4886 (1996); Phys. Rev. D **81**, 074024 (2010); T. Stelzer and S. Willenbrock, Phys. Lett. B **374**, 169 (1996); W. Bernreuther, A. Brandenburg and Z. G. Si, Phys. Rev. Lett. **87**, 242002 (2001); W. Bernreuther and Z. G. Si, Nucl. Phys. B **837**, 90 (2010). G. Mahlon, arXiv:1007.1716 [hep-ph].
- [13] For new physics contribution to top spin correlation, see, e.g., K. Cheung, Phys. Rev. D **55**, 4430 (1997); B. Holdom and T. Torma, Phys. Rev. D **60**, 114010 (1999); M. Arai, *et al.*, Phys. Rev. D **70**, 115015 (2004); Phys. Rev. D **75**, 095008 (2007); Acta Phys. Polon. B **40**, 93 (2009); M. Arai, N. Okada and K. Smolek, Phys. Rev. D **79**, 074019 (2009); C. X. Yue, T. T. Zhang and J. Y. Liu, J. Phys. G **37**, 075016 (2010).
- [14] S. Berge, W. Hollik, W. M. Mosle and D. Wackerroth, Phys. Rev. D **76**, 034016 (2007); Z. Sullivan, Phys. Rev. D **56**, 451 (1997) S. Alam, *et al.*, Phys. Rev. D **55**, 1307 (1997); C. S. Li, *et al.*, Phys. Rev. D **52**, 5014 (1995); Phys. Lett. B **379**, 135 (1996); Phys. Rev. D **52**, 1541 (1995); Phys. Rev. D **54**, 4380 (1996).
- [15] R. N. Mohapatra and J. C. Pati, Phys. Rev. D **11**, 2558 (1975). G. Senjanovic and R. N. Mohapatra, Phys. Rev. D **12**, 1502 (1975).
- [16] C. T. Hill, Phys. Lett. B **266**, 419 (1991); M. B. Popovic and E. H. Simmons, Phys. Rev. D **58**, 095007 (1998). R. S. Chivukula, H. Geogi and C. T. Hill, Phys. Rev. D **59**, 075003 (1999); K. Lane and E. Eichten, Phys. Lett. B **352**, 382 (1999); W. A. Bardeen, C. T. Hill and M. Lindner, Phys. Rev. D **41**, 1647 (1990); C. T. Hill and E. H. Simmons, Phys. Rept. **381**, 235 (2003).
- [17] D. Choudhury, R. M. Godbole, R. K. Singh and K. Wagh, Phys. Lett. B **657**, 69 (2007).
- [18] C. Amsler *et al.*, Particle Data Group, Phys. Lett. B **667**, 1 (2008).
- [19] J. Pumplin *et al.*, JHEP **0602**, 032 (2006).
- [20] T. Aaltonen *et al.* [The CDF Collaboration], Phys. Rev. D **82**, 052002 (2010) [arXiv:1002.2919 [hep-ex]].
- [21] T. Aaltonen *et al.* [CDF Collaboration], Phys. Rev. Lett. **102**, 222003 (2009).
- [22] For some early works on R -violating supersymmetry, see, e.g., L. Hall and M. Suzuki, Nucl.

- Phys. B **231**, 419 (1984); J. Ellis *et al.*, Phys. Lett. B **150**, 142 (1985); G. Ross and J. Valle, Phys. Lett. B **151**, 375 (1985); S. Dawson, Nucl. Phys. B **261**, 297 (1985); R. Barbieri and A. Masiero, Nucl. Phys. B **267**, 679 (1986); H. Dreiner and G.G. Ross, Nucl. Phys. B **365**, 597 (1991); J. Butterworth and H. Dreiner, Nucl. Phys. B **397**, 3 (1993).
- [23] For phenomenology of R -violation, see, e.g., V. Barger, G. F. Giudice, T. Han, Phys. Rev. D **40**, 2978 (1989); R. N. Mohapatra, Phys. Rev. D **34**, 3457 (1986); K. S. Babu, R. N. Mohapatra, Phys. Rev. Lett. **75**, 2276 (1995); G. Bhattacharyya, A. Raychaudhuri, Phys. Rev. D **57**, 3837 (1998); J. M. Yang, B.-L. Young, X. Zhang, Phys. Rev. D **58**, 055001 (1998); S. Bar-Shalom, G. Eilam, A. Soni, hep-ph/9812518; J. M. Yang, Eur. Phys. Jour. C **20**, 553 (2001); G. Eilam, *et al.*, Phys. Lett. B **510**, 227 (2001); G. Bhattacharyya, J. Ellis, K. Sridhar, Phys. Lett. B **355**, 193 (1995); Z. Heng *et al.*, Phys. Rev. D **79**, 094029 (2009). J. Erler, J. L. Feng, N. Polonsky, Phys. Rev. Lett. **78**, 3063 (1997); A. Datta, *et al.*, Phys. Rev. D **56**, 3107 (1997); R. J. Oakes *et al.*, Phys. Rev. D **57**, 534 (1998); J. L. Feng, J. F. Gunion, T. Han, Phys. Rev. D **58**, 071701 (1998); E. Perez, Y. Sirois, H. Dreiner, hep-ph/9703444; K. Hikasa, *et al.*, Phys. Rev. D **60**, 114041 (1999); A. Belyaev, *et al.*, JHEP 0409, 012 (2004); J. Cao, *et al.*, Phys. Rev. D **79**, 054003 (2009).
- [24] For a review of current bounds, see, e.g., D. Chang and W. Y. Keung, Phys. Lett. B **389**, 294 (1996). M. Chemtob, Prog. Part. Nucl. Phys. **54**, 71 (2005); R. Barbier *et al.*, Phys. Rept. **420**, 1 (2005).
- [25] P. Achard *et al.*, L3 Collaboration, Phys. Lett. B **580**, 37 (2004)
- [26] D. K. Ghosh, S. Raychaudhuri and K. Sridhar, Phys. Lett. B **396**, 177 (1997).
- [27] T. Aaltonen *et al.*, CDF Collaboration, arXiv: 0811.2512.
- [28] X. G. He and G. Valencia, Phys. Rev. D **66**, 013004 (2002); Phys. Rev. D **68**, 033011 (2003).
- [29] M. Cvetič and S. Godfrey, hep-ph/9504216; F. Abe *et al.* [CDF Collaboration], Phys. Rev. D **51**, 949 (1995); M. S. Carena, A. Daleo, B. A. Dobrescu and T. M. P. Tait, Phys. Rev. D **70**, 093009 (2004).
- [30] J. Erler, P. Langacker, S. Munir and E. R. Pena, JHEP **0908**, 017 (2009).
- [31] P. H. Frampton and S. L. Glashow, Phys. Lett. B **190**, 157 (1987). Phys. Rev. Lett. **58**, 2168 (1987).
- [32] V. Khachatryan *et al.* [CMS Collaboration], Phys. Rev. Lett. **105**, 211801 (2010).
- [33] F. Braam, M. Flossdorf, R. S. Chivukula, S. Di Chiara and E. H. Simmons, Phys. Rev. D **77**,

055005 (2008).

[34] F. Hubaut, *et al.*, Eur. Phys. J. C **44** 13 (2005).